Seeing the Light

PREASSEMBLY AND LIGAND-INDUCED CHANGES OF THE INTERFERON γ RECEPTOR COMPLEX IN CELLS*

Christopher D. Krause‡, Erwen Mei¶, Junxia Xie‡, Yiwei Jia§, Martin A. Bopp¶, Robin M. Hochstrasser¶, and Sidney Pestka‡‖

Our experiments were designed to test the hypothesis that the cell surface interferon γ receptor chains are preassembled rather than associated by ligand and to assess the molecular changes on ligand binding. To accomplish this, we used fluorescence resonance energy transfer, a powerful spectroscopic technique that has been used to determine molecular interactions and distances between the donor and acceptor. However, current commercial instruments do not provide sufficient sensitivity or the full spectra to provide decisive results of interactions between proteins labeled with blue and green fluorescent proteins in living cells. In our experiments, we used the blue fluorescent protein and green fluorescent protein pair, attached a monochrometer and charge-coupled device camera to a modified confocal microscope, reduced background fluorescence with the use of two-photon excitation, and focused on regions of single cells to provide clear spectra of fluorescence resonance energy transfer. In contrast to the prevailing view, the results demonstrate that the receptor chains are preassociated and that the intracellular domains move apart on binding the ligand interferon γ. Application of this technology should lead to new rapid methods for high throughput screening and delineation of the interactome of cells. ***Molecular & Cellular Proteomics 1:805–815, 2002.***

Specific protein-protein interactions are fundamental to most cellular functions, yet investigation of protein-protein interactions under physiological conditions has been problematic. Considerable effort has been made to identify these interactions. Typically these interactions have been detected by co-precipitation experiments in which an antibody to a known protein is mixed with a cell extract and used to precipitate the known protein and any proteins that are stably associated with it. However, the method does not yield data in real time in cells. Another approach has been to use an interaction trap system (the yeast two-hybrid system) to identify polypeptide sequences that bind to a predetermined polypeptide sequence present in a fusion protein in cells (1). As originally developed, the yeast two-hybrid system requires that both proteins to be tested be in the nucleus for the transcriptional activation to occur. To overcome this limitation, a method that does not involve transcription was developed to identify proteins that interact in the cytoplasm (2). In general, the two-hybrid method is used to identify novel polypeptide sequences that interact with a known protein (3–10). However, the two-hybrid systems do not permit real-time measurements of the interactions in cells.

Measurement of protein-protein interactions *in vivo* by noninvasive techniques can help to validate the physiological significance of the interactions and can also aid in identifying changes that occur in a cell or organism in response to physiological stimuli. One way to accomplish this is through fluorescence resonance energy transfer (FRET).[1] FRET is a powerful spectroscopic technique that has been used to determine protein-protein interactions and distances between two proteins in complexes (11, 12). In one example, we previously used FRET and fluorescence lifetime measurements to determine the distance between two regions of the ribosome (13). Very little is known about the physical association of specific receptor chains of multichain complexes and whether chains from one receptor type directly interact with another (14). Important answers should be provided by applying the FRET technique to cells.

FRET has begun to be used to determine interactions of proteins on the surface of cells. Monoclonal antibodies to cell surface receptors or other protein were labeled chemically with fluorescein isothiocyanate and Cy3 dyes. The *in vitro* fluorescent-labeled monoclonal antibodies directed against cell surface receptors were able to measure changes in the

From the ‡Department of Molecular Genetics, Microbiology and Immunology, Robert Wood Johnson Medical School-University of Medicine and Dentistry of New Jersey, Piscataway, New Jersey 08854, §Olympus America Inc., Melville, New York 11747-3157, and ¶Regional Laser and Biomedical Technology Laboratories, Department of Chemistry, University of Pennsylvania, Philadelphia, Pennsylvania 19104

Received, September 29, 2002, and in revised form, October 5, 2002

Published, MCP Papers in Press, October 5, 2002, DOI 10.1074/mcp.M200065-MCP200

[1] The abbreviations used are: FRET, fluorescence resonance energy transfer; CHO, Chinese hamster ovary; EBFP, enhanced blue fluorescent protein; EGFP, enhanced green fluorescent protein; FL, FLAG epitope; GFP, green fluorescent protein; BFP, blue fluorescent protein; IFN-γ, interferon γ; IFN-γR1, interferon γ receptor chain 1 (also noted as IFN-γRα chain); IFN-γR2, interferon γ receptor chain 2 (also noted as IFN-γRβ chain); IL-10, interleukin 10; IL-10R1, interleukin 10 receptor chain 1; IL-10R2, interleukin 10 receptor chain 2; *HLAB7*, human leukocyte antigen B7; Hu, human; MHC, major histocompatibility complex.

distance of the receptor components as a function of ligand concentrations (15–18). The cloning of green fluorescent protein (GFP) has allowed biologists to label proteins with the fluorescent GFP using genetic engineering (19, 20). The pituitary transcription factor (Pit-1) fused to BFP (BFP-Pit-1) was confirmed to interact with the protein c-Est-1 fused to GFP (GFP-Ets-1) by FRET, an association that was previously shown by co-immunoprecipitation (21). The association of Bcl-2 and Beclin fused to various mutants of GFP was determined by FRET (22). Additional reports in the last few years have begun to determine the association of proteins in cells with the use of GFP and BFP or cyan fluorescent protein and yellow fluorescent protein pairs (23–35). The use of fluorescence lifetime imaging microscopy can eliminate the need for spectral separation and problems in FRET (36) as we found previously by pure spectral methods (13) because fluorescence lifetime measurements permit calculation of distances between donor and acceptor fluorophores totally independent of FRET (11, 12). Another technique, fluorescence recovery after photobleaching, was used to demonstrate the interaction of Ras and Rap1 in cells (37). In our experiments, we used the BFP and GFP pair, attached a monochrometer and charge-coupled device camera to a modified confocal microscope, reduced background fluorescence with the use of two-photon excitation, and focused on regions of single cells to provide fluorescence spectra of selected regions that exhibit clear signatures of fluorescence energy transfer. Our experiments were applied to the interferon γ (IFN-γ) receptor complex to test the hypothesis that the receptor chains are preassociated and to assess the molecular changes on ligand binding.

Interferons initiate signal transduction through specific cell surface receptors (14, 38–40). IFN-γ binds to the IFN-γ receptor binding subunit (IFN-γR1; receptor chain 1), a species-specific cell surface transmembrane receptor chain (41, 42). A second transmembrane protein (IFN-γR2) (43–45) is required for signal transduction (Fig. 1). The overall objective of our efforts is to provide an improved method to detect protein-protein interactions under physiological conditions in live cells by using FRET and to determine effects of ligands and other agents on the interactions by examining the IFN-γ receptor complex in detail by FRET.

Although a great deal of information has accumulated about cell surface receptors from biochemical observations, no direct measurements of receptor structure have been made in cells in the presence and absence of ligand. In most cases, the models of multichain receptor complexes were deduced from a combination of cross-linking, immunoprecipitation of the constituent proteins, and delineation of the signal transduction events. For example, based on a wide variety of studies the commonly held opinion has been that ligands join surface receptor chains that are not associated prior to attachment of ligand (46–53). All these results were deduced from indirect measurements. However, some more recent observations have begun to suggest that receptor chains can be preassociated in the cell membrane (54–80). To provide a direct way to clarify the various models of receptor action, we established an approach to measure interactions of receptor chains in living cells. To assess the structure of the receptor chains and the effects of ligands directly, we used FRET and focused on the IFN-γ receptor. The chains and functions of the IFN-γ receptor complex have been defined in some detail over the past 2 decades (14, 39, 81–83). Indirect evidence exists about the structure of the IFN-γ receptor complex prior to its activation by IFN-γ. Most investigators have concluded that the IFN-γ receptor and other receptors are assembled after ligand binding because only then was optimal immunoprecipitation of both chains obtained with an antibody to IFN-γR1 (84–86). Accordingly, most models of the IFN-γ receptor consider it to consist of four chains: two IFN-γR1 and two IFN-γR2 chains, consistent with a large body of data. The ligand IFN-γ is a dimer that binds to two IFN-γR1 chains but does not directly bind to the IFN-γR2 chain in the absence of the IFN-γR1 chain. In the current model (Fig. 1), upon IFN-γR1 binding, the receptor chains associate to form a condensed complex that activates the Jak kinases that cross-phosphorylate each other. After binding of ligand, it was concluded that the chains of the IFN-γ receptor complex are brought together, and signal transduction is initiated by ligand binding (Fig. 1). Here we report the results of FRET in examining receptor structure directly and provide evidence for a new model of receptor structure and function.

EXPERIMENTAL PROCEDURES

Construction of Vectors to Measure FRET in Cells and Transfections—As noted above, GFP and BFP were discovered and developed by a number of groups (19, 20) who enabled these fluorescent proteins to be seen and localized in cells (19–35), and several groups have begun to use FRET to study the interactions of proteins in cells (21–35). In our studies, the IFN-γ receptor complex (Fig. 1) was used as the model system to evaluate the ability of FRET to provide insight into the structure of the receptor and to determine the molecular dynamics after attachment of the ligand IFN-γ to the receptor. To carry out these studies, IFN-γR1 and IFN-γR2 chains with EBFP (enhanced BFP cDNA optimized to contain mammalian codons) and GFP fused to the carboxyl termini of their intracellular domains were constructed (Fig. 2, *top*). EBFP, rather than BFP, was used for all constructions. By fusing the DNA encoding the EBFP to the DNA encoding the carboxyl terminus of the IFN-γR1 chain and by fusing the DNA encoding GFP to the DNA encoding the carboxyl terminus of the IFN-γR2 chain, the cells produce IFN-γR1/EBFP and IFN-γR2/GFP when these recombinant expression vectors are transfected into cells. In this way, the EBFP and GFP were fused to the intracellular domains of IFN-γR1 and IFN-γR2, respectively (Fig. 2) to monitor interactions among these two receptor chains in intact cells with and without IFN-γ treatment. All IFN-γR2 constructions contained the FLAG (FL) epitope as noted in the figure legends. The detailed construction of FL-IFN-γR2/γR2 (first γR2 represents extracellular domain and second γR2 represents intracellular domain) was described in detail elsewhere (87, 88). It differs from the wild type IFN-γR2 sequence in the following ways: the FLAG epitope was placed between the end of the putative signal peptide sequence and the putative beginning of the extracellular domain, and an *Nhe*I site was

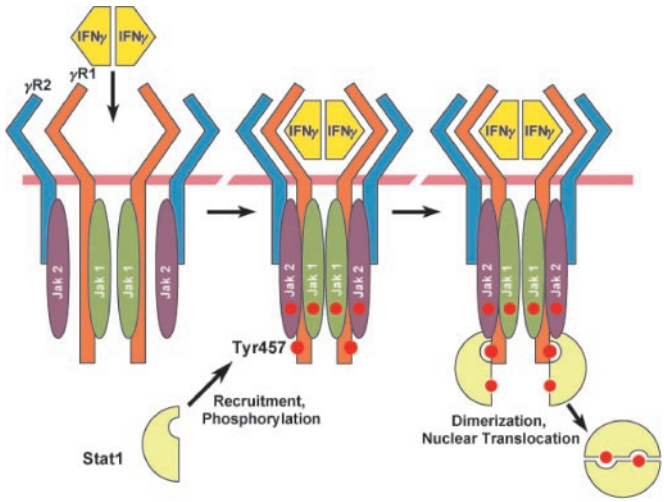

FIG. 1. **Traditional model of the IFN-γ receptor complex.** The IFN-γ receptor complex consists of two different chains, IFN-γR1 and IFN-γR2 (14, 42, 44, 45, 82, 91, 93–95). The ligand IFN-γ is a dimer that binds to two IFN-γR1 chains but does not directly bind to the IFN-γR2 chain in the absence of the IFN-γR1 chain. In the current model, upon IFN-γR1 binding, the receptor chains associate to form a condensed complex that activates the Jak kinases that cross-phosphorylate each other (*solid circles*). The activated Jak kinases then phosphorylate tyrosine 457 of each IFN-γR1 chain that serves as the recruitment site for Stat1α, which in turn is phosphorylated by the Jak kinases. Once phosphorylated, the phosphorylated Stat1α proteins detach from each IFN-γR1 chain and then dimerize to form the transcription factor that is translocated to the nucleus to activate IFN-γ-regulated genes.

engineered into the beginning of the transmembrane domain, producing a three-amino acid mutation. Neither change affected the function of IFN-γR2. Because it was necessary to have cells express two proteins labeled with EBFP and GFP at similar levels, we used a single vector expressing both proteins for transfection rather than co-transfection with two vectors. Thus, tandem vectors, in which transcription of each cDNA is controlled by its own separate promoter and polyadenylation signal on a single plasmid, were constructed as described previously (88). The plasmid harboring the IFN-γR1 chain (or the IL-10R1 chain) was digested at the 3′ end with *Mlu*I and at the 5′ end with *Bgl*II. The large fragment, encoding the IFN-γR1 cDNA and its expression elements, was retained. The plasmid harboring the FL-IFN-γR2 chain (or the FL-IL-10R2 chain) was digested with *Bgl*II at its 5′ end and *Bss*HII at its 3′ end. The larger fragment, retaining the FL-IFN-γR2 cDNA and its expression elements, was retained. Ligation of the cohesive ends yielded tandem vectors. To prepare EBFP or GFP fusion products, the segments encoding EBFP or GFP were amplified by PCR from appropriate vectors (89, 90) and then fused to the vectors expressing FL-IFN-γR2, IFN-γR1, or IL-10R2 with EBFP or GFP attached to the 3′ terminus of the expression construct to make FL-IFN-γR2/EBFP, FL-IFN-γR2/GFP, IFN-γR1/EBFP, and IL-10R2/GFP, respectively. Schematic illustrations of the resultant EBFP- and GFP-labeled receptor chains are shown in Figs. 2 and 3. Transient transfections in COS-1 cells by the DEAE-dextran protocol (91) were used for all experiments except where noted. Stable transformants were made in the Chinese hamster ovary (CHO)-derived cell line q3 by the Lipofectin method and limiting dilution clonal isolation. The derivation of the CHO q3 cell line is described in the legend to Fig. 3.

Analysis of FRET between Receptor Chains in Single Cells: FRET and Equipment Used—To demonstrate GFP and EBFP fluorescence and FRET, a confocal microscope was modified to include a monochrometer associated with a back illumination liquid nitrogen-cooled charge-coupled device camera so that fluorescence emission spectra could be obtained from illuminated cells. The S65T variant of GFP with an excitation maximum at 488 nm was used in all our studies (92). The enhanced GFP (EGFP) optimized for mammalian codons has the same excitation and emission maxima as GFP (S65T), 488 and 509 nm, respectively. We used GFP rather than EGFP in these experiments because EGFP was not available at the time we began the constructions. Single-photon excitation at 488 nm of the GFP with an argon laser delivering 0.5 microwatt at the sample yielded the signature GFP emission having a maximum at 509 nm. The BFP and EBFP have excitation and emission maxima at 380 nm and 445 nm, respectively. Because we found that excitation at 380 of cells produced very high background fluorescence, we used two-photon excitation to substantially reduce the sample excitation volume along with quartz cover slides, which resulted in a significantly decreased background fluorescence. The infrared light produced little or no cellular damage compared with ultraviolet light. To excite the EBFP at its excitation maximum of 380 nm, a pulsed femtosecond mode-locked infrared Ti:sapphire laser (2 milliwatts) was tuned to 760 nm. As illustrated in the *lower part* of Fig. 2, two-photon excitation (760 nm) of EBFP effectively excites the protein at it is maximum absorption at 380 nm to produce an emission spectrum with a maximum at 445 nm. If FRET occurs between EBFP and GFP, then the emission maximum of GFP at 509 nm will be observed.

Images, Spectra, and Activity of Human IFN-γR2/GFP and IFN-γR1/EBFP Transfected into Cells—The constructs expressing IFN-γR2/GFP and IFN-γR2/EBFP were individually transfected into COS-1 cells, and images were taken with a camera attached to a confocal microscope. The images show that both IFN-γR2/GFP (Fig. 4, *top left*) and IFN-γR2/EBFP (Fig. 4, *top right*) were visualized by epifluorescence after transfection upon exciting the IFN-γR2/GFP at 488 and the IFN-γR2/EBFP at 380 nm. Similar images were obtained for IFN-γR1/EBFP (not shown). To demonstrate that each of the constructs was functional, vectors expressing IFN-γR2/GFP or IFN-γR1/EBFP were transfected into CHO cells expressing the complementary human chain (44, 82, 91). MHC Class I induction by IFN-γ demonstrated that each chain was functional (data not shown). To demonstrate that the constructs were functional when transfected together into cells, a tandem vector coexpressing IFN-γR2/GFP and IFN-γR1/EBFP was transfected into Chinese hamster ovary cells expressing none of the human IFN-γ receptor chains (CHO q3). The MHC Class I surface antigen induction in response to IFN-γ in CHO q3 cells expressing IFN-γR2/GFP and IFN-γR1/EBFP (Fig. 3, *right panels*) shows that both receptor chains are functional. Similar activity measurements with other receptor chains such as IFN-γR2/EGFP, IFN-γR2/EBFP, and FL-IL-10R2/GFP demonstrated that all these receptor chains with fluorescent proteins fused to their carboxyl termini were functional.

RESULTS

The carboxyl-terminal end of the intracellular domain of the two chains of the human IFN-γ receptor complex, Hu-IFN-γR1 and Hu-IFN-γR2, were fused to EBFP and GFP, respectively (Fig. 2). In addition, the carboxyl-terminal end of the intracellular domain of the IL-10R2 chain was fused to GFP as a control. To ascertain that the receptor chains with GFP and EBFP (Fig. 3, *right panel*) were functional, these chains were transfected into CHO q3 cells to determine whether they could function as well as the same chains without the fluo-

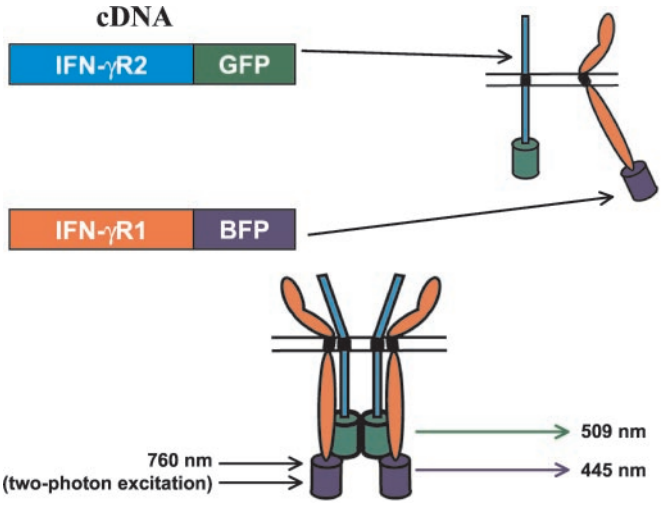

FIG. 2. **Schematic of fluorescence transfer between blue and green fluorescent proteins fused to IFN-γR1 and IFN-γR2 chains.** EBFP and GFP were fused to the IFN-γR1 and IFN-γR2 chains shown in the *upper portion* of the figure and described under "Experimental Procedures." Because the cellular background was high when the EBFP was excited with blue light at 380 nm, infrared light at 760 nm was used to excite the EBFP with two photons. With no fluorescence transfer, the excitation of the EBFP will emit light with a maximum at 445 nm. If fluorescence transfer from EBFP to GFP occurs, the maximum wavelength of the emitted light will be seen at 509 nm.

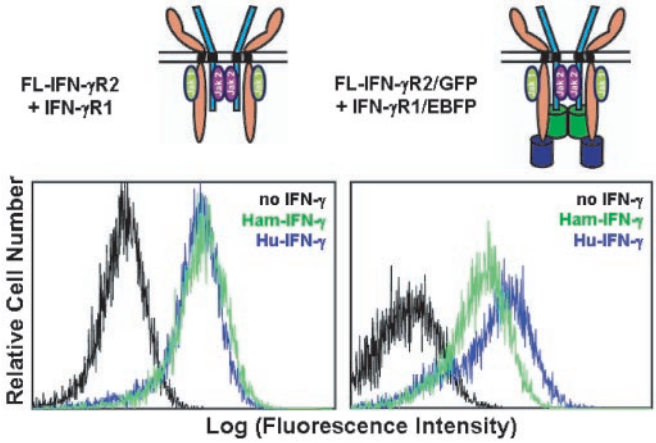

FIG. 3. **Fluorescent receptor chains are functional.** The human receptor chains (IFN-γR1 and FL-IFN-γR2) without fluorescent proteins (*left panel*) and those with the fluorescent proteins (IFN-γR1/EBFP and FL-IFN-γR2/GFP) (*right panel*) were transfected into CHO q3 cells, and MHC Class I antigen induction was measured in response to hamster and human IFN-γ. In the absence of the human receptor chains, Hu-IFN-γ has no effect on CHO cells (82, 91, 102). The hamster IFN-γ was used as a positive control to show that the CHO cells can propagate IFN-γ signaling. The CHO q3 cells were derived as follows. Hamster UCH-12 cells containing a stable translocation of human chromosome 3q were obtained from Carol Jones and David Patterson. UCH-12 cells were transfected with plasmid pJY150R1.1 that encodes the intact *HLAB7* gene (104), and the resulting cells were designated q3. This hamster cell line, derived from CHO-K1, does not express Hu-IFN-γR1 or Hu-IFN-γR2 and can reconstitute signaling in response to Hu-IFN-γ only when both chains are expressed in these cells. The stably transfected population of q3 cells was grown in F12 medium supplemented with 10% fetal bovine serum without selecting antibiotics. Selection was performed by sorting of 2% of cells exhibiting the greatest fluorescence in an MHC Class I assay after 3 days of treatment with Hu-IFN-β. After three rounds of selection, individual clones were isolated by limiting dilution and amplified. Clones were isolated that induced significantly higher levels of MHC Class I surface antigen in response to hamster IFN-γ. From these clones, one clone (designated q3) was chosen that possessed a high efficiency of transfection with a plasmid encoding Hu-IFN-γR1 and Hu-IFN-γR2 and exhibited expression of reconstituted human IFN-γ receptor complexes assayed by MHC Class I surface antigen induction of the geneticin-resistant transfected population in response to Hu-IFN-γ. MHC Class I antigen induction in response to IFN-γ was performed as described previously (82). *Ham*, hamster.

rescent proteins (Fig. 3, *left panel*). The results show that MHC Class I antigen induction in response to human IFN-γ was as effective as that of hamster IFN-γ, demonstrating that the receptor chains with or without GFP and EBFP were functional. Cells were transfected with the IFN-γR2/EBFP and IFN-γR2/GFP separately to establish that the chains fused to EBFP and GFP, respectively, provided the expected fluorescence signatures. The spectral signature of GFP and EBFP was seen in cells expressing IFN-γR2/GFP (Fig. 4, *left panels*; excited at 488 nm) and IFN-γR2/EBFP (Fig. 4, *right panels*; excited at 380 nm). Identical spectral signatures were observed in cells expressing IFN-γR1/EBFP and IFN-γR2/BFP (data not shown). Thus the data showed that both IFN-γR2/EBFP and IFN-γR2/GFP provided the expected spectral signatures (Fig. 4). However, there was substantial background fluorescence when EBFP was excited at 380 nm so that we used two-photon excitation (760 nm) to minimize this in the subsequent FRET assays.

We next prepared transient transfectants in COS-1 cells expressing matched (Hu-IFN-γR1 and Hu-IFN-γR2) and mismatched (Hu-IFN-γR1 and Hu-IL-10R2) receptor pairs (Fig. 5). The matched pair, Hu-IFN-γR1/EBFP and Hu-IFN-γR2/GFP, represents the two chains of the Hu-IFN-γ receptor complex. The mismatched pair represents two chains from similar receptor complexes, Hu-IFN-γR1/EBFP and Hu-IL-10R2/GFP, but are not known to interact. FRET was measured upon excitation at 760 nm in cells expressing each of these pairs of receptor chains in the absence of ligand (Fig. 6). The spectrum of cells expressing the mismatched pair Hu-IFN-γR1/EBFP and Hu-IL-10R2/GFP shows the blue (EBFP) spectrum together with background fluorescence, demonstrating little or no interaction of these receptor chains. In contrast, the matched pair, Hu-IFN-γR1/EBFP and Hu-IFN-γR2/GFP, excited at 760 nm exhibits the fluorescence emission signature of the GFP, demonstrating clear transfer between the EBFP and GFP proteins. The distance between the intracellular regions of IFN-γR1/EBFP and IFN-γR2/GFP chains was calculated (13) to be 36 Å, whereas the distance between the Hu-IFN-γR1/EBFP and

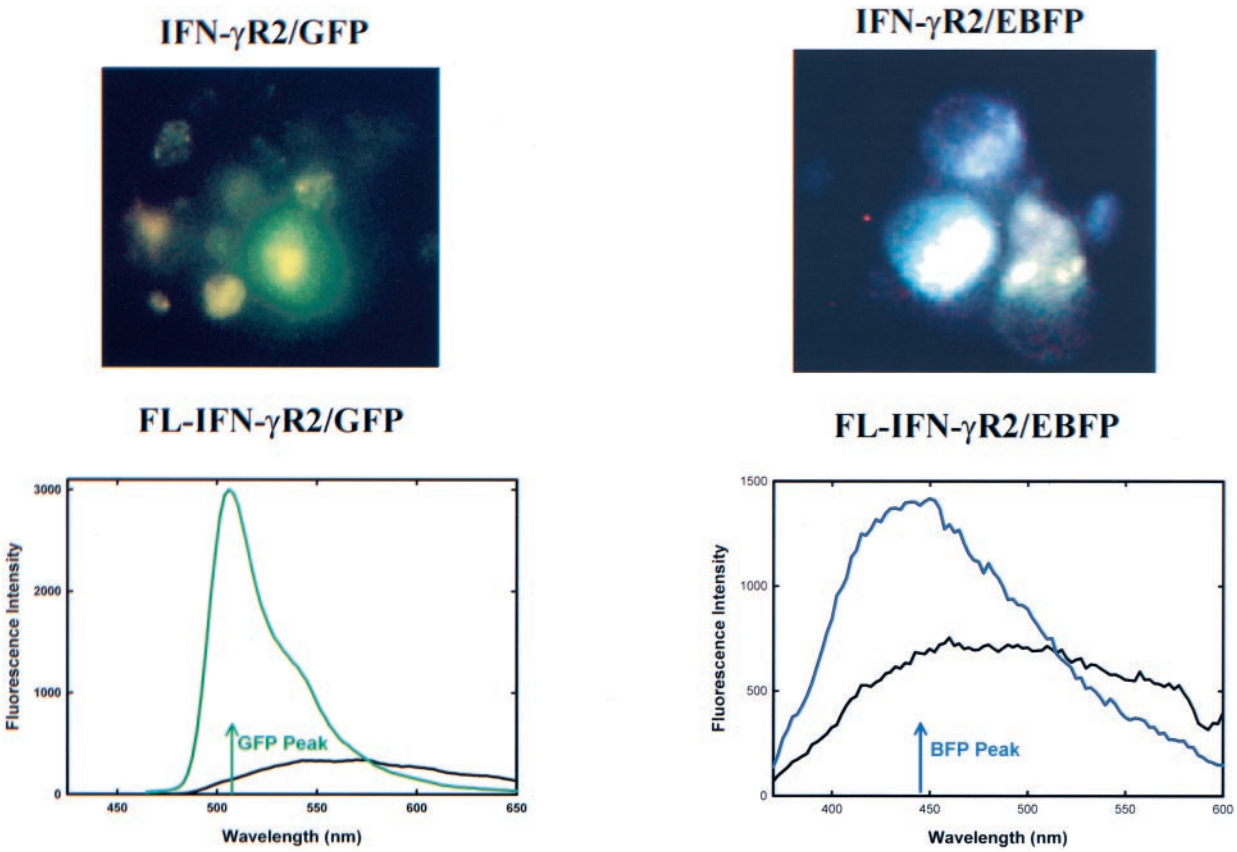

FIG. 4. **The fluorescent receptor chains exhibit their characteristic fluorescent signatures: images and spectra of human IFN-γR2/GFP and IFN-γR2/EBFP transfected into cells.** FL-IFN-γR2/GFP and FL-IFN-γR2/EBFP were each separately transfected into COS cells. A camera was used with the confocal microscope to obtain the images for human IFN-γR2/GFP (*top left*) and IFN-γR2/EBFP (*top right*) in COS-1 cells. Similar images were obtained for IFN-γR1/BFP and IFN-γR1/EBFP (not shown). The spectral signatures of GFP (*green*) and EBFP (*blue*) can be seen in COS-1 cells expressing FL-IFN-γR2/GFP and FL-IFN-γR2/EBFP (*lower left* and *right*, respectively). The *black curves* represent the relative epifluorescence of the cells in the absence of the respective transfected fluorescent receptor chains.

Hu-IL-10R2/GFP was not measurable.[2] Thus, the IFN-γR1 and IFN-γR2 chains are preassociated prior to ligand binding as demonstrated by the significant FRET and the GFP signature with maximum of about 509 nm on excitation at 760 nm. Addition of the ligand IFN-γ to cells expressing the mismatched pair IFN-γR1/EBFP and IL-10R2/GFP did not affect the spectrum (Fig. 7). The spectra were virtually identical in the presence or absence of IFN-γ. In contrast, the effect of IFN-γ on the FRET of the matched receptor pair expressed in cells showed that IFN-γ produced a change in the spectrum, causing a major reduction in the FRET compared with the FRET in the absence of IFN-γ (Fig. 8). The distance between the intracellular regions of Hu-IFN-γR1/EBFP and Hu-IFN-γR2/GFP chains in the absence and presence of ligand was calculated (13) to be 36 and 63 Å, respectively. Therefore, the intracellular domains of the IFN-γR1/EBFP and IFN-γR2/GFP chains move apart on addition of ligand.

Because the IFN-γ receptor complex consists of four chains, we examined the effect of ligand on cells expressing only the IFN-γR2 chain (IFN-γR2/EBFP and IFN-γR2/GFP), but no IFN-γR1 chain, in the presence and absence of ligand (Fig. 9, *left panels*). In the absence of ligand, FRET was demonstrated between these two IFN-γR2 chains. There was no

[2] These distances are values of R obtained from $R = R_0 (I_D f_A / I_A)^{1/6}$ where I_D and I_A are the observed BFP and GFP fluorescence signals, f_A is the GFP fluorescence yield, and R_0 is the Forster radius for the GFP/BFP pair. The fluorescence signal may originate from a spatially unresolved set of sources that could include some receptors with only BFP as well as those complexes having a distribution of GFP/BFP distances and angles. Therefore the R values should be considered as estimates of the upper limits of the mean separations in the complexes. Furthermore, we cannot exclude the possibility that some or all of the decrease in FRET can be attributed to a change in the orientation of the donor and acceptor fluorophores caused by a change in the orientation but not the average distance between the intracellular domains. Since we cannot measure the orientation of the fluorophores with respect to each other, the calculations and conclusions assumed no change in the orientation of the fluorophores on ligand binding. Nevertheless, a change in the structure of the IFN-γ receptor complex is unequivocally observed by the change in the FRET after addition of IFN-γ to cells. Although this change is assumed to be a result of changes in distance, the change in FRET observed could be due in whole or part to a rotation of receptor chains after interaction with ligand.

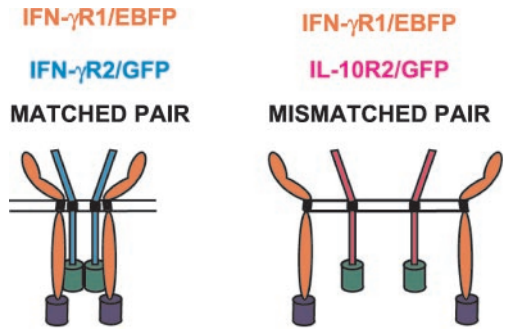

FIG. 5. **Illustration of matched (FL-IFN-γR2/GFP and IFN-γR1/EBFP) and mismatched (IFN-γR1/EBFP and FL-IL-10R2/GFP) pairs of receptors.** The matched pair, FL-IFN-γR2/GFP and FL-IFN-γR1/EBFP, are the two chains of the IFN-γ receptor complex fused to GFP and EBFP, respectively. The mismatched pair, IFN-γR1/EBFP and FL-IL-10R2/GFP, are the first chain of the IFN-γ receptor complex and the second chain of the IL-10 receptor complex, fused to EBFP and GFP, respectively.

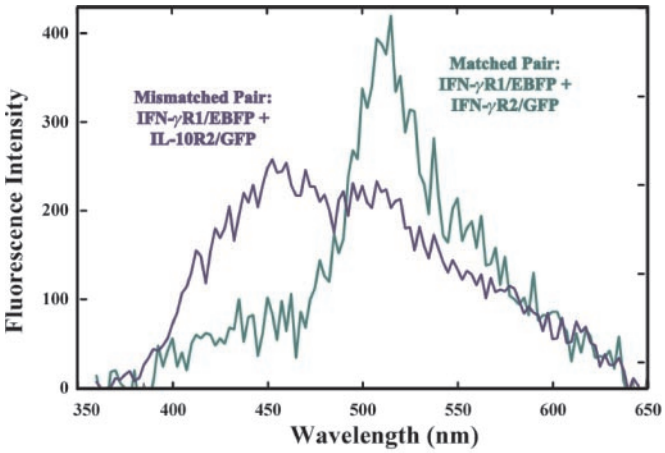

FIG. 6. **Comparison of fluorescence emission spectra of cells expressing the matched and mismatched pair of receptor chains.** The matched receptor chains are FL-IFN-γR2/GFP and IFN-γR1/EBFP (*green curve*); the mismatched receptor chains are IFN-γR1/EBFP and FL-IL-10R2/GFP (*blue curve*). The fluorescence emission spectra in response to two-photon excitation at 760 nm are shown.

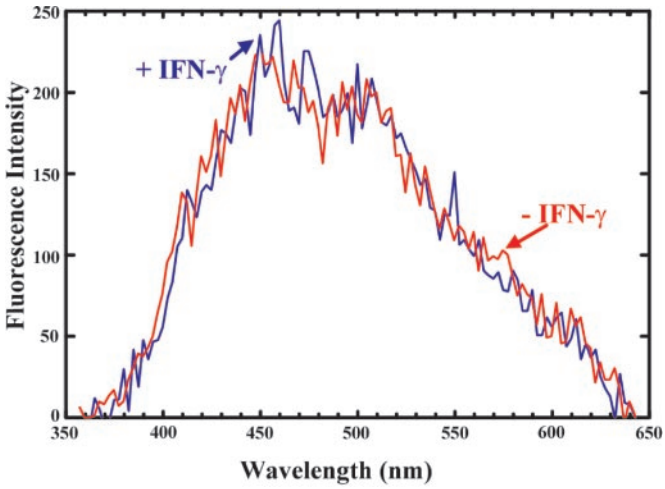

FIG. 7. **Comparison of fluorescence spectra of cells expressing the mismatched pair of receptor chains in the presence and absence of IFN-γ.** The mismatched receptor chains are IFN-γR1/EBFP and FL-IL-10R2/GFP. The spectrum in *red* was taken in the absence of IFN-γ. IFN-γ was then added to the medium, and the spectrum was taken (*blue curve*) of the same region in the same cell. The fluorescence emission spectra in response to two-photon excitation at 760 nm are shown.

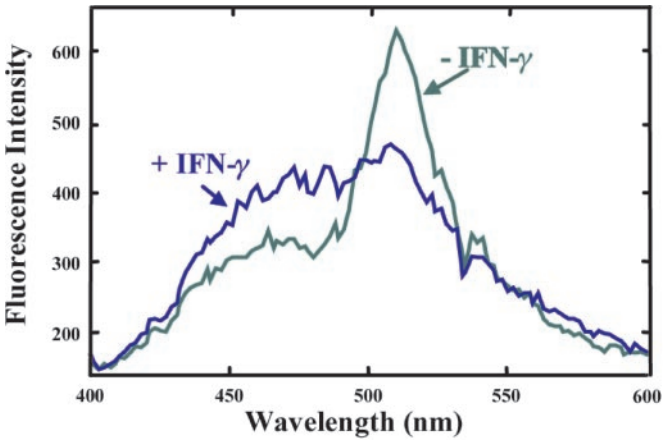

FIG. 8. **Comparison of fluorescence spectra of cells expressing the matched pair of receptor chains in the presence and absence of IFN-γ.** The matched receptor chains are FL-IFN-γR2/GFP and IFN-γR1/EBFP. The spectrum in *green* was taken in the absence of IFN-γ. IFN-γ (3500 units/ml) was then added to the medium, and the spectrum was taken (*blue curve*) of the same region in the same cell. The fluorescence emission spectra in response to two-photon excitation at 760 nm are shown.

change in the spectrum in the presence of IFN-γ. This demonstrated that the IFN-γR2 chains are preassociated even in the absence of the IFN-γR1 chains. Furthermore, this observation that IFN-γ did not alter the spectrum and, therefore, the distance between the IFN-γR2 chains is consistent with previous experiments that showed that IFN-γ did not produce any measurable signal transduction in cells expressing only the IFN-γR2 chain (44, 45, 82, 91, 93, 94). When the spectra were measured in cells expressing both IFN-γR2/EBFP and IFN-γR2/GFP chains together with the IFN-γR1 chain without a fluorescent tag (Fig. 9, *right panels*), it was apparent that addition of the ligand IFN-γ changed the spectrum. In the absence of ligand, the spectrum was qualitatively similar in cells expressing IFN-γR2/EBFP and IFN-γR2/GFP whether the IFN-γR1 chain was present or not (Fig. 9, *cf. left* and *right panels*). However, in the presence of IFN-γ there was a large change in the spectrum of cells expressing IFN-γR2/EBFP, IFN-γR2/GFP, and IFN-γR1 chains (Fig. 9, *right panel*). The results demonstrate that the IFN-γR2 chains are preassociated independently of the presence of the IFN-γR1 chain but that the IFN-γR1 chain is required for the IFN-γR2 chains to move apart in response to IFN-γ. This result is consistent with previous reports that demonstrated that both chains are re-

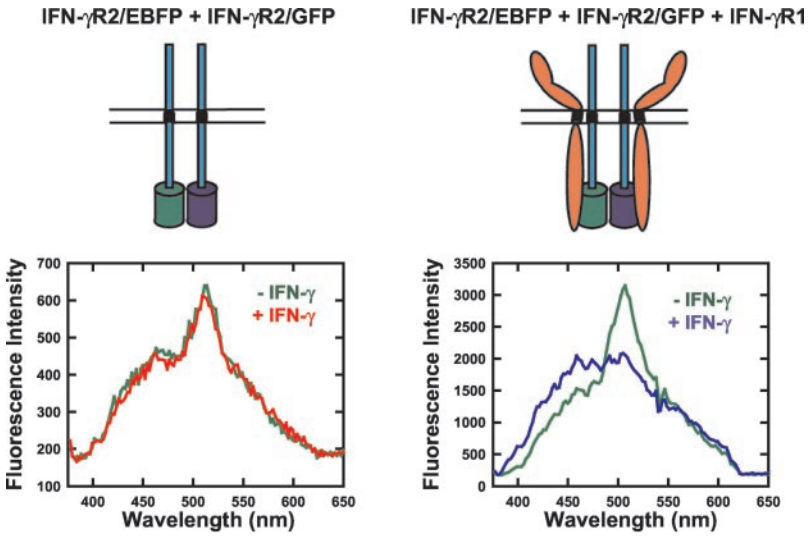

FIG. 9. **Comparison of fluorescence spectra of cells expressing the FL-IFN-γR2/EBFP and FL-IFN-γR2/GFP chains in the presence and absence of the IFN-γR1 chain and in the presence and absence of ligand.** COS-1 cells were transfected with FL-IFN-γR2/EBFP and FL-IFN-γR2/GFP without transfection with IFN-γR1 (*left panels*). COS-1 cells were also transfected with IFN-γR2/EBFP and IFN-γR2/GFP together with the IFN-γR1 chain (*right panels*). The spectra of the COS-1 cells transfected with the FL-IFN-γR2/EBFP and FL-IFN-γR2/GFP in the presence and absence of IFN-γ and in the presence and absence of the IFN-γR1 chain are shown in the panels. In all experiments with FRET, measurements were taken at 15 min after addition of IFN-γ when noted. All laser excitation experiments were performed with single cells, although multiple cells were sampled and provided similar results. The fluorescence emission spectra in response to two-photon excitation at 760 nm are shown.

quired for signal transduction (14, 42, 44, 45, 82, 91, 93–95). However, it appears that in the presence of the IFN-γR1 chain, the IFN-γR2/EBFP and IFN-γR2/GFP chains are somewhat closer because there is an increase in FRET in the presence of the IFN-γR1 chain (Fig. 9, *cf*. *left* and *right panels*).

A model of the IFN-γ receptor complex that is consistent with the data is shown in Fig. 10. In the absence of ligand (Fig. 10, *left panel*), the intracellular domains of the receptor chains are close to one another, preventing signal transduction as the intracellular components necessary for signaling are prevented from entering the receptor complex by the close proximity of the intracellular domains of these chains. Upon binding of the ligand IFN-γ, the intracellular domains of the receptor chains move apart, opening the area for multiple molecules required for signal transduction to enter the receptor complex (Fig. 10, *right panel*).

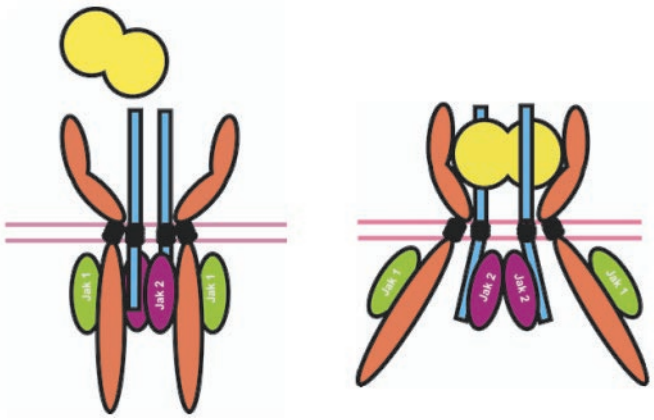

FIG. 10. **Model of the change in receptor structure on engagement of the ligand IFN-γ.** When IFN-γ binds to the receptor complex, the distance between the IFN-γR1 and IFN-γR2 chains and the distance between the two IFN-γR2 chains increases. Opening the intracellular domain regions provides an opportunity for entry of components of the downstream signal transduction components. The distances and the changes in distances shown are not proportional to the actual measurements.

DISCUSSION

Attempts have been made to assess interactions among the receptor chains by indirect methods; however, except for cross-linking, each method was dependent upon relatively high affinity associations after disruption of the cell. Standard procedures such as immunoprecipitation, cross-linking, size-exclusion chromatography, analytical ultracentrifugation, and laser light scattering were used to investigate the interaction between the two IFN-γR1 chains and immunoprecipitation and cross-linking between the IFN-γR1 and IFN-γR2 chains before and after addition of IFN-γ. Soluble IFN-γR1 and cell surface membrane-bound IFN-γR1 was not observed to dimerize in the absence of IFN-γ (86, 96–100). However, it was reported that IFN-γR1 and IFN-γR2 chains co-precipitated with antibodies against the IFN-γR2 before and after addition of IFN-γ (101). In those experiments digitonin, which does not disrupt detergent-resistant micelles, was used to disrupt cellular membranes during the immunoprecipitation procedures, leaving open the possibility that proteins associated with the detergent-resistant micelles could be co-pre-

cipitated nonspecifically. In fact, it was later confirmed that disruption of cells with digitonin yielded co-immunoprecipitation of IFN-γR1 and IFN-γR2 chains, but the authors noted that use of the ionic detergent Brij-96, which disrupts detergent-resistant micelles, avoided nonspecific co-immunoprecipitations and, at the same time, disrupted the interaction between IFN-γR1 and IFN-γR2 chains prior to addition of IFN-γ (84). They and others (84, 86), who used ionic detergents to disrupt cells, concluded that the IFN-γR1 and IFN-γR2 chains are not preassociated in the cell membrane prior to addition of the ligand IFN-γ on the basis that co-precipitation of these chains occurred only after IFN-γ was present, results that led to the current accepted model shown in Fig. 1 that indicates that the receptor chains do not associate until the ligand is present. The techniques used to measure protein-protein interactions often remove the proteins from the context of the superstructure of the membranes and other cellular components of which they are an integral part. Thus, high affinity interactions, but not low affinity interactions, can be measured by these procedures. In contrast, the use of FRET permits the direct visualization of all these interactions in cells. Association constants that are too weak to be observed in solution after disruption of cells can be clearly seen by FRET (Figs. 6, 8, and 9) because the receptors are anchored in the membrane.

The effective association constant in solution of two molecules each with two distinct binding sites for association is the product of the association constants for each site times 55, the molarity of water, assuming no conformational constraints. Thus, two low affinity sites can produce an overall high association constant for the molecules. The fact that both receptor chains are anchored in the membrane provides a high affinity site for each, also keeping them at an effective high concentration in the plasma membrane. Furthermore, quantitative measurement of the distances between the fluorescent chains measured helps to avoid artifacts and eliminate nonspecific interactions because only distances less than 100 Å can be observed by FRET with current technology. Thus, when anchored, binding of proteins with relatively low affinity in solution can be visualized clearly by a real-time technique that can measure FRET in live cells. Accordingly, we believe the association of the IFN-γR1 and IFN-γR2 chains and other receptor chain pairs has often been missed by the usual assays that measure these interactions after they have been removed from the membrane. This is likely due to the fact that the binding constants of the interactions of the extracellular and/or intracellular domains are probably very low. However, once the receptors are anchored in the membrane, weak interactions take place because the association constant of the two chains in the membrane is a function of the product of the association constant of the membrane binding component and the receptor chain component. Once dissociated from the membrane, the receptor chains have little or no affinity for each other in the absence of ligand. This decrease in entropy of the anchored system increases the likelihood of interactions on the membrane and allows even weak interactions to occur. This phenomenon is used to explain the use of solid surfaces as catalysts in chemical reactions as well as increased avidity of polyvalent compounds for their targets compared with monovalent compounds. These results have ramifications for all proteins and other components of cells. Indeed, we predict this technology will permit the definition of the interactions of many proteins in living cells in real time. Proteins that require additional components to interact in cells will be able to be discerned even though the soluble purified proteins do not appear to associate.

The results demonstrate directly that the receptor chains of the IFN-γ receptor complex are preassembled on the cell membrane. Furthermore, the data prove that the receptor complex consists of four (or possibly more chains) because both the IFN-γR1 and IFN-γR2 pair (Figs. 6 and 8) and the IFN-γR2 and IFN-γR2 pair (Fig. 9) are preassociated. It is also evident from the data that the IFN-γR2 and IFN-γR2 chains are preassociated in the absence of the IFN-γR1 chain but that the presence of the IFN-γR1 brings the IFN-γR2 and IFN-γR2 chains closer together (Fig. 9). IFN-γ has no effect on the separation of IFN-γR2 chains in the absence of the IFN-γR1 chain (Fig. 9, *left panel*) in accord with previous reports that IFN-γ does not bind to the IFN-γR2 chain and that IFN-γ exhibits no activity in the presence of the IFN-γR2 chain only (42, 44, 82, 91, 93, 102, 103). We suggest that this paradigm is likely to be applicable to other receptor chains and that receptor chains are preassociated in cells ready for activation by ligand. This conclusion leads to the deduction that cell surface receptor chains have specific sites, receptor association regions, that enable them to associate. Moreover, the increase in distance between the intracellular regions of the receptor chains opens the receptor complexes for the attachment of the signal transduction components that are excluded from the receptor complexes until ligand engagement. Thus, our direct measurements of the distances between the IFN-γ receptor chains before and after engagement of ligand suggest a new paradigm for receptor structure and function.

Because FRET is a real-time technique, changes in protein-protein interactions or protein positions in complexes in live cells can be determined over the course of time or modulation of the system being analyzed. Because relatively little is known about the physical association of specific receptor chains of multichain complexes and whether chains from one receptor type directly interact with those from another type (14), the use of FRET to determine this should provide an answer to these questions by applying the technique to cells. Furthermore, such studies can be extended to the downstream signal transduction events in response to ligand by determining the order, interactions, and kinetics of these processes. This information will permit the development of pharmaceuticals that can interfere with IFN-γ signaling by interfering with IFN-γ binding to the complex, by blocking the

activation of the ligand-receptor complex, or by altering downstream signal transduction events. The protein pairs used in the FRET assays would be adjusted accordingly to measure these specific events. In addition, this technology can be adapted to screen small molecule drugs by a quantitative, sensitive, and rapid real-time assay. A major goal will be to use this technology to study the interaction of receptor chains and of many other proteins in cells under physiological conditions. Ultimately, this strategy could permit delineation of the entire proteome map of any cell, the interactome.

The ability to accomplish this efficiently will have major ramifications for analyzing protein-protein interactions, ligand-receptor interactions, signal transduction, and many other cellular processes. Furthermore, questions relevant to protein interactions in cells that have been addressed indirectly should be able to be answered definitively with direct measurements and the time course of the events determined. The overall objective of our efforts is to provide an improved method to detect protein-protein interactions under physiological conditions in live cells by using FRET and to determine effects of ligands and other agents on the interactions by examining the IFN-γ receptor complex in detail by FRET. The results will have many useful applications in understanding receptor structure and will provide a basis for high throughput screening of receptor ligands in single living cells.

Acknowledgments—We thank Ellen Feibel and Eleanor Kells for assistance with the preparation of this manuscript. We thank Ralph A. Bradshaw for sharing reference searches and comments, Roger Tsien for the cDNAs encoding GFP variants, Carol Jones and David Patterson for the hamster UCH-12 cells, and Dolph Hatfield for many comments and suggestions to improve the text.

* This study was supported in part by United States Public Health Services Grants RO1-CA46465 from NCI, National Institutes of Health; RO1-AI36450, RO1-AI43369, and 2T32AI07403 from NIAID, National Institutes of Health (to S. P.); and an award from the Milstein Family Foundation (to S. P.). The costs of publication of this article were defrayed in part by the payment of page charges. This article must therefore be hereby marked "*advertisement*" in accordance with 18 U.S.C. Section 1734 solely to indicate this fact.

‖ To whom correspondence should be addressed: Dept. of Molecular Genetics, Microbiology, and Immunology, Robert Wood Johnson Medical School, 675 Hoes Lane, Piscataway, NJ 08854-5635. Tel.: 732-235-4567; Fax: 732-235-5223; E-mail: Pestka@umdnj.edu.

REFERENCES

1. Fields, S., and Song, O. (1989) A novel genetic system to detect protein-protein interactions. *Nature* **340,** 245–246
2. Aronheim, A., Zandi, E., Hennemann, H., Elledge, S. J., and Karin, M. (1997) Isolation of an AP-1 repressor by a novel method for detecting protein-protein interactions. *Mol. Cell. Biol.* **17,** 3094–3102
3. Bartel, P., Chien, C. T., Sternglanz, R., and Fields, S. (1993) Elimination of false positives that arise in using the two-hybrid system. *BioTechniques* **14,** 920–924
4. Durfee, T., Becherer, K., Chen, P.-L., Yeh, S.-H., Yang, Y., Kilburn, A., Lee, W.-H., and Elledge, S. J. (1993) The retinoblastoma protein associates with the protein phosphatase type 1 catalytic subunit. *Genes Dev.* **7,** 555–569
5. Hardy, C. F., Sussel, L., and Shore, D. (1992) A RAP1-interacting protein involved in transcriptional silencing and telomere length regulation. *Genes Dev.* **6,** 801–814
6. Luban, J., Bossolt, K. L., Franke, E. K., Kalpana, G. V., and Goff, S. P. (1993) Human immunodeficiency virus type 1 Gag protein binds to cyclophilins A and B. *Cell* **73,** 1067–1078
7. Vojtek, A. B., Hollenberg, S. M., and Cooper, J. A. (1993) Mammalian ras interacts directly with the serine/threonine kinase raf. *Cell* **74,** 205–214
8. Yang, X., Hubbard, E. J. A., and Carlson, M. (1992) A protein kinase substrate identified by the two-hybrid system. *Science* **257,** 680–682
9. Pollack, B. P., Kotenko, S. V., He, W., Izotova, L. S., Barnoski, B. L., and Pestka, S. (1999) The human homologue of the yeast proteins Skb1 and Hsl7p interacts with Jak kinases and contains protein methyltransferase activity. *J. Biol. Chem.* **274,** 31531–31542
10. Sarkar, S., Pollack, B. P., Lin, K. T., Kotenko, S. V., Cook, J. R., Lewis, A., and Pestka, S. (2001) hTid-1, a human DnaJ protein, modulates the interferon signaling pathway. *J. Biol. Chem.* **276,** 49034–49042
11. Cantor, C. R., and Schimmel, P. R. (1980) *Biophysical Chemistry Part II: Techniques for the Study of Biological Structure and Function*, W. H. Freeman & Company, New York
12. van der Meer, B. W., Coker, G., and Simon, S.-Y. (1994) *Resonance Energy Transfer: Theory and Data*, Wiley, John & Sons, Incorporated, New York
13. Langlois, R., Lee, C. C., Cantor, C. R., Vince, R., and Pestka, S. (1976) The distance between two functionally significant regions of the 50S Escherichia coli ribosome: the erythromycin binding site and proteins L7/L12. *J. Mol. Biol.* **106,** 297–313
14. Pestka, S., Kotenko, S. V., Muthukumaran, G., Izotova, L. S., Cook, J. R., and Garotta, G. (1997) The interferon γ (IFN-γ) receptor: a paradigm for the multichain cytokine receptor. *Cytokine Growth Factor Rev.* **8,** 189–206
15. Broudy, V. C., Lin, N. L., Buhring, H. J., Komatsu, N., and Kavanagh, T. J. (1998) Analysis of c-kit receptor dimerization by fluorescence resonance energy transfer. *Blood* **91,** 898–906
16. Damjanovich, S., Bene, L., Matko, J., Alileche, A., Goldman, C. K., Sharrow, S., and Waldmann, T. A. (1997) Preassembly of interleukin 2 (IL-2) receptor subunits on resting Kit 225 K6 T cells and their modulation by IL-2, IL-7, and IL-15: a fluorescence resonance energy transfer study. *Proc. Natl. Acad. Sci. U. S. A.* **94,** 13134–13139
17. Guo, C., Dower, S. K., Holowka, D., and Baird, B. (1995) Fluorescence resonance energy transfer reveals interleukin (IL)-1-dependent aggregation of IL-1 type I receptors that correlates with receptor activation. *J. Biol. Chem.* **270,** 27562–27568
18. Kenworthy, A. K., and Edidin, M. (1998) Distribution of a glycosylphosphatidylinositol-anchored protein at the apical surface of MDCK cells examined at a resolution of <100 Å using imaging fluorescence resonance energy transfer. *J. Cell Biol.* **142,** 69–84
19. Heim, R., Prasher, D. C., and Tsien, R. Y. (1994) Wavelength mutations and posttranslational autoxidation of green fluorescent protein. *Proc. Natl. Acad. Sci. U. S. A.* **91,** 12501–12504
20. Prasher, D. C. (1995) Using GFP to see the light. *Trends Genet.* **11,** 320–323
21. Day, R. N. (1998) Visualization of Pit-1 transcription factor interactions in the living cell nucleus by fluorescence resonance energy transfer microscopy. *Mol. Endocrinol.* **12,** 1410–1419
22. Gordon, G. W., Berry, G., Liang, X. H., Levine, B., and Herman, B. (1998) Quantitative fluorescence resonance energy transfer measurements using fluorescence microscopy. *Biophys. J.* **74,** 2702–2713
23. Janetopoulos, C., Jin, T., and Devreotes, P. (2001) Receptor-mediated activation of heterotrimeric G-proteins in living cells. *Science* **291,** 2408–2411
24. Li, H. Y., Ng, E. K., Lee, S. M., Kotaka, M., Tsui, S. K., Lee, C. Y., Fung, K. P., and Waye, M. M. (2001) Protein-protein interaction of FHL3 with FHL2 and visualization of their interaction by green fluorescent proteins (GFP) two-fusion fluorescence resonance energy transfer (FRET). *J. Cell. Biochem.* **80,** 293–303
25. Llopis, J., Westin, S., Ricote, M., Wang, Z., Cho, C. Y., Kurokawa, R., Mullen, T. M., Rose, D. W., Rosenfeld, M. G., Tsien, R. Y., Glass, C. K., and Wang, J. (2000) Ligand-dependent interactions of coactivators steroid receptor coactivator-1 and peroxisome proliferator-activated receptor binding protein with nuclear hormone receptors can be imaged in live cells and are required for transcription. *Proc. Natl. Acad. Sci. U. S. A.* **97,** 4363–4368

26. Mahajan, N. P., Linder, K., Berry, G., Gordon, G. W., Heim, R., and Herman, B. (1998) Bcl-2 and Bax interactions in mitochondria probed with green fluorescent protein and fluorescence resonance energy transfer. *Nat. Biotechnol.* **16,** 547–552
27. Margolin, W. (2000) Green fluorescent protein as a reporter for macromolecular localization in bacterial cells. *Methods* **20,** 62–72
28. Mizuno, H., Sawano, A., Eli, P., Hama, H., and Miyawaki, A. (2001) Red fluorescent protein from Discosoma as a fusion tag and a partner for fluorescence resonance energy transfer. *Biochemistry* **40,** 2502–2510
29. Overton, M. C., and Blumer, K. J. (2000) G-protein-coupled receptors function as oligomers in vivo. *Curr. Biol.* **10,** 341–344
30. Pollok, B. A., and Heim, R. (1999) Using GFP in FRET-based applications. *Trends Cell Biol.* **9,** 57–60
31. Prufer, K., Racz, A., Lin, G. C., and Barsony, J. (2000) Dimerization with retinoid X receptors promotes nuclear localization and subnuclear targeting of vitamin D receptors. *J. Biol. Chem.* **275,** 41114–41123
32. Schmid, J. A., Birbach, A., Hofer-Warbinek, R., Pengg, M., Burner, U., Furtmuller, P. G., Binder, B. R., and de Martin, R. (2000) Dynamics of NFκB and IκBα studied with green fluorescent protein (GFP) fusion proteins. Investigation of GFP-p65 binding to DNA by fluorescence resonance energy transfer. *J. Biol. Chem.* **275,** 17035–17042
33. Sorkin, A., McClure, M., Huang, F., and Carter, R. (2000) Interaction of EGF receptor and grb2 in living cells visualized by fluorescence resonance energy transfer (FRET) microscopy. *Curr. Biol.* **10,** 1395–1398
34. Vanderklish, P. W., Krushel, L. A., Holst, B. H., Gally, J. A., Crossin, K. L., and Edelman, G. M. (2000) Marking synaptic activity in dendritic spines with a calpain substrate exhibiting fluorescence resonance energy transfer. *Proc. Natl. Acad. Sci. U. S. A.* **97,** 2253–2258
35. Xia, Z., Zhou, Q., Lin, J., and Liu, Y. (2001) Stable SNARE complex prior to evoked synaptic vesicle fusion revealed by fluorescence resonance energy transfer. *J. Biol. Chem.* **276,** 1766–1771
36. Harpur, A. G., Wouters, F. S., and Bastiaens, P. I. (2001) Imaging FRET between spectrally similar GFP molecules in single cells. *Nat. Biotechnol.* **19,** 167–169
37. Mochizuki, N., Yamashita, S., Kurokawa, K., Ohba, Y., Nagai, T., Miyawaki, A., and Matsuda, M. (2001) Spatio-temporal images of growth-factor-induced activation of Ras and Rap1. *Nature* **411,** 1065–1068
38. Langer, J. A., and Pestka, S. (1988) Interferon receptors. *Immunol. Today* **9,** 393–400
39. Pestka, S., Langer, J. A., Zoon, K. C., and Samuel, C. E. (1987) Interferons and their actions. *Annu. Rev. Biochem.* **56,** 727–777
40. Pestka, S. (1997) The interferon receptors. *Semin. Oncol.* **24,** Suppl. 9, S9-18–S9-40
41. Mariano, T. M., Kozak, C. A., Langer, J. A., and Pestka, S. (1987) The mouse immune interferon receptor gene is located on chromosome 10. *J. Biol. Chem.* **262,** 5812–5814
42. Rashidbaigi, A., Langer, J. A., Jung, V., Jones, C., Morse, H. G., Tischfield, J. A., Trill, J. J., Kung, H.-F., Pestka, S., and Kung, H. F. (1986) The gene for the human immune interferon receptor is located on chromosome 6. *Proc. Natl. Acad. Sci. U. S. A.* **83,** 384–388
43. Hibino, Y., Mariano, T. M., Kumar, C. S., Kozak, C. A., and Pestka, S. (1991) Expression and reconstitution of a biologically active mouse interferon γ receptor in hamster cells: chromosomal location of an accessory factor. *J. Biol. Chem.* **266,** 6948–6951
44. Jung, V., Rashidbaigi, A., Jones, C., Tischfield, J. A., Shows, T. B., and Pestka, S. (1987) Human chromosomes 6 and 21 are required for sensitivity to human interferon γ. *Proc. Natl. Acad. Sci. U. S. A.* **84,** 4151–4155
45. Jung, V., Jones, C., Rashidbaigi, A., Geyer, D. D., Morse, H. G., Wright, R. B., and Pestka, S. (1988) Chromosome mapping of biological pathways by fluorescence-activated cell sorting and cell fusion: the human interferon γ receptor as a model system. *Somat. Cell Mol. Genet.* **14,** 583–592
46. Youssoufian, H., Longmore, G., Neumann, D., Yoshimura, A., and Lodish, H. F. (1993) Structure, function, and activation of the erythropoietin receptor. *Blood* **81,** 2223–2236
47. Lemmon, M. A., Bu, Z., Ladbury, J. E., Zhou, M., Pinchasi, D., Lax, I., Engelman, D. M., and Schlessinger, J. (1997) Two EGF molecules contribute additively to stabilization of the EGFR dimer. *EMBO J.* **16,** 281–294
48. Watowich, S. S., Yoshimura, A., Longmore, G. D., Hilton, D. J., Yoshimura, Y., and Lodish, H. F. (1992) Homodimerization and constitutive activation of the erythropoietin receptor. *Proc. Natl. Acad. Sci. U. S. A.* **89,** 2140–2144
49. Watowich, S. S., Hilton, D. J., and Lodish, H. F. (1994) Activation and inhibition of erythropoietin receptor function: role of receptor dimerization. *Mol. Cell. Biol.* **14,** 3535–3549
50. Yarden, Y., and Schlessinger, J. (1987) Self-phosphorylation of epidermal growth factor receptor: evidence for a model of intermolecular allosteric activation. *Biochemistry* **26,** 1434–1442
51. Yarden, Y., and Schlessinger, J. (1987) Epidermal growth factor induces rapid, reversible aggregation of the purified epidermal growth factor receptor. *Biochemistry* **26,** 1443–1451
52. Zhou, M., Felder, S., Rubinstein, M., Hurwitz, D. R., Ullrich, A., Lax, I., and Schlessinger, J. (1993) Real-time measurements of kinetics of EGF binding to soluble EGF receptor monomers and dimers support the dimerization model for receptor activation. *Biochemistry* **32,** 8193–8198
53. Weiss, A., and Schlessinger, J. (1998) Switching signals on or off by receptor dimerization. *Cell* **94,** 277–280
54. Baer, K., Al Hasani, H., Parvaresch, S., Corona, T., Rufer, A., Nolle, V., Bergschneider, E., and Klein, H. W. (2001) Dimerization-induced activation of soluble insulin/IGF-1 receptor kinases: an alternative mechanism of activation. *Biochemistry* **40,** 14268–14278
55. Bishayee, S., Majumdar, S., Khire, J., and Das, M. (1989) Ligand-induced dimerization of the platelet-derived growth factor receptor. Monomer-dimer interconversion occurs independent of receptor phosphorylation. *J. Biol. Chem.* **264,** 11699–11705
56. Bouvier, M. (2001) Oligomerization of G-protein-coupled transmitter receptors. *Nat. Rev. Neurosci.* **2,** 274–286
57. Brennan, P. J., Kumagai, T., Berezov, A., Murali, R., Greene, M. I., and Kumogai, T. (2000) HER2/neu: mechanisms of dimerization/oligomerization. *Oncogene* **19,** 6093–6101
58. Chan, F. K., Chun, H. J., Zheng, L., Siegel, R. M., Bui, K. L., and Lenardo, M. J. (2000) A domain in TNF receptors that mediates ligand-independent receptor assembly and signaling. *Science* **288,** 2351–2354
59. Chow, D., Ho, J., Nguyen Pham, T. L., Rose-John, S., and Garcia, K. C. (2001) In vitro reconstitution of recognition and activation complexes between interleukin-6 and gp130. *Biochemistry* **40,** 7593–7603
60. Devi, L. A. (2001) Heterodimerization of G-protein-coupled receptors: pharmacology, signaling and trafficking. *Trends Pharmacol. Sci.* **22,** 532–537
61. Gadella, T. W., Jr., and Jovin, T. M. (1995) Oligomerization of epidermal growth factor receptors on A431 cells studied by time-resolved fluorescence imaging microscopy. A stereochemical model for tyrosine kinase receptor activation. *J. Cell Biol.* **129,** 1543–1558
62. Gamett, D. C., Pearson, G., Cerione, R. A., and Friedberg, I. (1997) Secondary dimerization between members of the epidermal growth factor receptor family. *J. Biol. Chem.* **272,** 12052–12056
63. Raffioni, S., Zhu, Y. Z., Bradshaw, R. A., and Thompson, L. M. (1998) Effect of transmembrane and kinase domain mutations on fibroblast growth factor receptor 3 chimera signaling in PC12 cells. A model for the control of receptor tyrosine kinase activation. *J. Biol. Chem.* **273,** 35250–35259
64. Guimond, A., Sulea, T., Zwaagstra, J. C., Ekiel, I., and O'Connor-McCourt, M. D. (2002) Identification of a functional site on the type I TGF-β receptor by mutational analysis of its ectodomain. *FEBS Lett.* **513,** 147–152
65. Jiang, G., and Hunter, T. (1999) Receptor signaling: when dimerization is not enough. *Curr. Biol.* **9,** R568–R571
66. Johannessen, L. E., Haugen, K. E., Ostvold, A. C., Stang, E., and Madshus, I. H. (2001) Heterodimerization of the epidermal-growth-factor (EGF) receptor and ErbB2 and the affinity of EGF binding are regulated by different mechanisms. *Biochem. J.* **356,** 87–96
67. Kan, M., Wu, X., Wang, F., and McKeehan, W. L. (1999) Specificity for fibroblast growth factors determined by heparan sulfate in a binary complex with the receptor kinase. *J. Biol. Chem.* **274,** 15947–15952
68. Maher, D. W., Strawn, L. M., and Donoghue, D. J. (1993) Alanine mutagenesis of conserved residues in the platelet-derived growth factor family: identification of residues necessary for dimerization and transformation. *Oncogene* **8,** 533–541
69. Martin-Fernandez, M., Clarke, D. T., Tobin, M. J., Jones, S. V., and Jones,

G. R. (2002) Preformed oligomeric epidermal growth factor receptors undergo an ectodomain structure change during signaling. *Biophys. J.* **82,** 2415–2427
70. McInnes, C., and Sykes, B. D. (1997) Growth factor receptors: structure, mechanism, and drug discovery. *Biopolymers* **43,** 339–366
71. Moriki, T., Maruyama, H., and Maruyama, I. N. (2001) Activation of preformed EGF receptor dimers by ligand-induced rotation of the transmembrane domain. *J. Mol. Biol.* **311,** 1011–1026
72. Morrow, M. R., and Grant, C. W. (2000) The EGF receptor transmembrane domain: peptide-peptide interactions in fluid bilayer membranes. *Biophys. J.* **79,** 2024–2032
73. Sako, Y., Minoghchi, S., and Yanagida, T. (2000) Single-molecule imaging of EGFR signalling on the surface of living cells. *Nat. Cell Biol.* **2,** 168–172
74. Siegel, R. M., Frederiksen, J. K., Zacharias, D. A., Chan, F. K., Johnson, M., Lynch, D., Tsien, R. Y., and Lenardo, M. J. (2000) Fas preassociation required for apoptosis signaling and dominant inhibition by pathogenic mutations. *Science* **288,** 2354–2357
75. van den Akker, F. (2001) Structural insights into the ligand binding domains of membrane bound guanylyl cyclases and natriuretic peptide receptors. *J. Mol. Biol.* **311,** 923–937
76. Wang, F., Kan, M., McKeehan, K., Jang, J. H., Feng, S., and McKeehan, W. L. (1997) A homeo-interaction sequence in the ectodomain of the fibroblast growth factor receptor. *J. Biol. Chem.* **272,** 23887–23895
77. Watowich, S. S. (1999) Activation of erythropoietin signaling by receptor dimerization. *Int. J. Biochem. Cell Biol.* **31,** 1075–1088
78. Wiesmann, C., Muller, Y. A., and de Vos, A. M. (2000) Ligand-binding sites in Ig-like domains of receptor tyrosine kinases. *J. Mol. Med.* **78,** 247–260
79. Wilson, I. A., and Jolliffe, L. K. (1999) The structure, organization, activation and plasticity of the erythropoietin receptor. *Curr. Opin. Struct. Biol.* **9,** 696–704
80. Wiseman, P. W., and Petersen, N. O. (1999) Image correlation spectroscopy. II. Optimization for ultrasensitive detection of preexisting platelet-derived growth factor-beta receptor oligomers on intact cells. *Biophys. J.* **76,** 963–977
81. Aguet, M., Dembic, Z., and Merlin, G. (1988) Molecular cloning and expression of the human interferon-γ receptor. *Cell* **55,** 273–280
82. Soh, J., Donnelly, R. J., Kotenko, S., Mariano, T. M., Cook, J. R., Wang, N., Emanuel, S. L., Schwartz, B., Miki, T., and Pestka, S. (1994) Identification and sequence of an accessory factor required for activation of the human interferon γ receptor. *Cell* **76,** 793–802
83. Darnell, J. E., Jr., Kerr, I. M., and Stark, G. R. (1994) Jak-STAT pathways and transcriptional activation in response to IFNs and other extracellular signaling proteins. *Science* **264,** 1415–1421
84. Bach, E. A., Tanner, J. W., Marsters, S., Ashkenazi, A., Aguet, M., Shaw, A. S., and Schreiber, R. D. (1996) Ligand-induced assembly and activation of the γ interferon receptor in intact cells. *Mol. Cell. Biol.* **16,** 3214–3221
85. Ishiharu, C., Ochiai, K., Kagami, M., Matsuyama, G., Koya, N., and Tomioka, H. (1998) Interferon-γ receptor β-chain expression and formation of α- and β-chain complexes after receptor conjugation on human peripheral eosinophils. *Int. Arch. Allergy Immunol.* **117,** Suppl. 1, 72–76
86. Kotenko, S. V., Izotova, L. S., Pollack, B. P., Mariano, T. M., Donnelly, R. J., Muthukumaran, G., Cook, J. R., Garotta, G., Silvennoinen, O., Ihle, J. N., and Pestka, S. (1995) Interaction between the components of the interferon γ receptor complex. *J. Biol. Chem.* **270,** 20915–20921
87. Kotenko, S. V., Izotova, L. S., Pollack, B. P., Muthukumaran, G., Paukku, K., Silvennoinen, O., Ihle, J. N., and Pestka, S. (1996) Other kinases can substitute for jak2 in signal transduction by IFN-γ. *J. Biol. Chem.* **271,** 17174–17182
88. Kotenko, S. V., Krause, C. D., Izotova, L. S., Pollack, B. P., Wu, W., and Pestka, S. (1997) Identification and functional characterization of a second chain of the interleukin-10 receptor complex. *EMBO J.* **16,** 5894–5903
89. Heim, R., Cubitt, A. B., and Tsien, R. Y. (1995) Improved green fluorescence. *Nature* **373,** 663–664
90. Heim, R., and Tsien, R. Y. (1996) Engineering green fluorescent protein for improved brightness, longer wavelengths and fluorescence resonance energy transfer. *Curr. Biol.* **6,** 178–182
91. Jung, V., Jones, C., Kumar, C. S., Stefanos, S., O'Connell, S., and Pestka, S. (1990) Expression and reconstitution of a biologically active human interferon γ receptor in hamster cells. *J. Biol. Chem.* **265,** 1827–1830
92. Ormo, M., Cubitt, A. B., Kallio, K., Gross, L. A., Tsien, R. Y., and Remington, S. J. (1996) Crystal structure of the Aequorea victoria green fluorescent protein. *Science* **273,** 1392–1395
93. Hemmi, S., Bohni, R., Stark, G., Di Marco, F., and Aguet, M. (1994) A novel member of the interferon receptor family complements functionality of the murine interferon γ receptor in human cells. *Cell* **76,** 803–810
94. Lembo, D., Ricciardi-Castagnoli, P., Alber, G., Ozmen, L., Landolfo, S., Bluthmann, H., Dembic, Z., Kotenko, S. V., Cook, J. R., Pestka, S., and Garotta, G. (1996) Mouse macrophages carrying both subunits of the human interferon-γ (IFN-γ) receptor respond to human IFN-γ but do not acquire full protection against viral cytopathic effect. *J. Biol. Chem.* **271,** 32659–32666
95. Pestka, S. (2000) The human interferon α species and receptors. *Biopolymers* **55,** 254–287
96. Fountoulakis, M., Juranville, J.-F., Maris, A., Ozmen, L., and Garotta, G. (1990) One interferon γ receptor binds one interferon γ dimer. *J. Biol. Chem.* **265,** 19758–19767
97. Fountoulakis, M., Juranville, J.-F., Stuber, D., Weibel, E. K., and Garotta, G. (1990) Purification and biochemical characterization of a soluble human interferon γ receptor expressed in *Escherichia coli*. *J. Biol. Chem.* **265,** 13268–13275
98. Fountoulakis, M., Zulauf, M., Lusting, A., and Garotta, G. (1992) Stoichiometry of interaction between interferon γ and its receptor. *Eur. J. Biochem.* **208,** 781–787
99. Greenlund, A. C., Schreiber, R. D., Goeddel, D. V., and Pennica, D. (1993) Interferon-γ induces receptor dimerization in solution and on cells. *J. Biol. Chem.* **268,** 18103–18110
100. Krause, C. D., Lunn, C. A., Izotova, L. S., Mirochnitchenko, O., Kotenko, S. V., Lundell, D. J., Narula, S. K., and Pestka, S. (2000) Signaling by covalent heterodimers of interferon-γ. Evidence for one-sided signaling in the active tetrameric receptor complex. *J. Biol. Chem.* **275,** 22995–23004
101. Sakatsume, M., Igarashi, K., Winestock, K. D., Garotta, G., Larner, A. C., and Finbloom, D. S. (1995) The Jak kinases differentially associate with the α and β (accessory factor) chains of the interferon γ receptor to form a functional receptor unit capable of activating STAT transcription factors. *J. Biol. Chem.* **270,** 17528–17534
102. Cook, J. R., Emanuel, S. L., Donnelly, R. J., Soh, J., Mariano, T. M., Schwartz, B., Rhee, S., and Pestka, S. (1994) Sublocalization of the human interferon-γ receptor accessory factor gene and characterization of accessory factor activity by yeast artificial chromosomal fragmentation. *J. Biol. Chem.* **269,** 7013–7018
103. Soh, J., Donnelly, R. J., Mariano, T. M., Cook, J. R., Schwartz, B., and Pestka, S. (1993) Identification of a yeast artificial chromosome clone encoding an accessory factor for the human interferon γ receptor: evidence for multiple accessory factors. *Proc. Natl. Acad. Sci. U. S. A.* **90,** 8737–8741
104. Barbosa, J. A., Kamarck, M. E., Biro, P. A., Weissman, S. M., and Ruddle, F. H. (1982) Identification of human genomic clones coding the major histocompatibility antigens HLA-a2 and HLA-B7 by DNA-mediated gene transfer. *Proc. Natl. Acad. Sci. U. S. A.* **79,** 6327–6331